Journal of Catalysis **203,** 201–212 (2001)
doi:10.1006/jcat.2001.3308, available online at http://www.idealibrary.com on IDEAL®

Influence of Pore and Crystal Size of Crystalline Titanosilicates on Phenol Hydroxylation in Different Solvents

Uwe Wilkenhöner,* Gunther Langhendries,† Frederik van Laar,‡ Gino V. Baron,† David W. Gammon,§
Pierre A. Jacobs,‡ and Eric van Steen*,[1]

*Catalysis Research Unit, Department of Chemical Engineering, University of Cape Town, Private Bag, Rondebosch 7701, South Africa; †Department of Chemical Engineering, Vrije Universiteit Brussel, Pleinlaan 2, B-1050 Brussel, Belgium; ‡Centre for Surface Chemistry and Catalysis, Katholieke Universiteit Leuven, Kasteelpark Arenberg 23, B-3001 Heverlee, Belgium; and §Department of Chemistry, University of Cape Town, Private Bag, Rondebosch 7701, South Africa

Received April 2, 2001; revised June 15, 2001; accepted June 19, 2001

The hydroxylation of phenol into catechol and hydroquinone with aqueous H_2O_2 (30%) and titanium-substituted molecular sieves (TS-1 and Al-free Ti-Beta) was investigated to understand the role of the zeolite structure, the crystal size, the external surface of the zeolite, and the nature of the solvent on the product selectivity. Comparing Al-free Ti-Beta and TS-1 samples with similar pore lengths, the activity as well as the ratio of catechol to hydroquinone was significantly higher for Al-free Ti-Beta, showing diffusional constraints for the conversion of phenol and geometric constraints for the formation of catechol. The diffusional constraints in the conversion of phenol were confirmed by using small crystallites of TS-1. The role of the external surface of TS-1 in the phenol hydroxylation was investigated by inertization of the external surface, using cycles of low-temperature chemical vapor deposition (CVD) of tetraethoxysilane followed by high-temperature calcination. Consecutive CVD cycles led to a slight increase of the selectivity toward hydroquinone for all tested solvents as well as a reduction of the coke formation in methanol and water. The ratio of hydroquinone to catechol, however, did not change much, indicating that catechol must also be formed inside the pore structure. A kinetic analysis of the reaction data with the parent and surface-inertized TS-1 revealed that the role of the external surface in terms of both activity and selectivity is significant and dependent on the solvent used. A reaction mechanism consistent with the observed enhanced selectivity for hydroquinone in protic solvents is proposed. © 2001 Academic Press

Key Words: **phenol hydroxylation; solvent effect; Al-free Ti-Beta; TS-1; CVD; silanization; kinetic analysis; sorption.**

1. INTRODUCTION

Over the past 20 years, numerous reports on the synthesis and application of titanium-substituted silicates have been published. In particular, titanium silicalite-1 (TS-1) was shown to be an active catalyst in the epoxidation of propylene and higher α-olefins, in the ammoximation of cyclohexanone, and in the hydroxylation of phenol. The hydroxylation of phenol yielding hydroquinone and catechol using aqueous hydrogen peroxide has been commercialized by Enichem (1). Several parameters such as calcination conditions (2), nature of solvent (3), temperature (4), and procedure for H_2O_2 addition (5) have been identified as key parameters. However, even today, various aspects of the phenol hydroxylation, such as the reaction mechanism, contribution of the external surface, and diffusion of the reactants and products, are not yet fully understood.

According to van der Pol *et al.* (6) phenol hydroxylation is governed by intracrystalline diffusion in large crystals of TS-1. These authors excluded a major influence of external surface activity. On the other hand, Tuel *et al.* (3) concluded that the product ratio of hydroquinone to catechol is mainly controlled by the external surface activity. Hydroquinone and catechol are thought to be the preferred reaction products in the micropores of TS-1 and on the external surface titanium sites, respectively.

The initial objective of this work was to gain further insight into the mechanism(s) controlling product selectivity. To achieve this, the influence of the pore structure, the crystal size, and the contribution of the external surface of titanium silicalite-1 to overall reaction parameters, such as phenol conversion, hydroquinone selectivity, and tar formation, were investigated in different solvents such as water, methanol, and acetone.

The contribution of the external surface can be investigated by eliminating the active sites located on the external surface of TS-1 by cyclic chemical vapor deposition (CVD) with tetraethoxysilane (TEOS) (7). The chemical vapor deposition of silanes on zeolitic aluminosilicates, especially ZSM-5, is a well-established technique to inertize the acid sites on the external surface (8). The inertization may lead to improvement in selectivity toward the product with the

---

[1] To whom correspondence should be addressed. Fax: +27-21-689 7579. E-mail: evs@chemeng.uct.ac.za.

0021-9517/01 $35.00

smallest kinetic diameter, as was observed in the toluene disproportionation to benzene and xylenes over H-ZSM-5. With increasing number of cycles the *p*-xylene content in the fraction of xylenes increases up to 99%, which was explained in terms of pore mouth narrowing (7).

TS-1 has a three-dimensional pore structure with pore dimensions of 5.6 × 5.4 Å while the larger pore molecular sieve Ti-beta has a two-dimensional pore structure with pore dimensions of 7.6 × 6.4 Å. Thus, the two materials can be used to investigate the influence of the pore geometry on the product selectivity and to identify shape-selective effects induced by the zeolite channels.

2. MATERIALS AND METHODS

2.1. Synthesis and Modification of Titanium-Containing Molecular Sieves

The titanium-substituted zeolites used in this work were two TS-1 samples with different crystal sizes and aluminium-free zeolite Ti-Beta. Small crystallites of TS-1 were synthesized (Si/Ti = 34) according to the method described by Tangaraj *et al.* (4). In a typical synthesis, 24.4 g of tetraethylorthosilicate (TEOS, Aldrich) was hydrolyzed with 29.3 g of tetrapropylammonium hydroxide solution (TPAOH, 20% in H_2O, Alfa). A solution of 1.23 g of tetrabutylorthotitanate (TBOT, Alfa) in 5.55 g of dry isopropanol (Merck) was then added dropwise. Subsequently, 9.8 g of TPAOH and 22.76 g of deionized water were added. Before autoclaving, the reaction mixture was heated to 80°C to remove the alcohol. The molar composition of the initial mixture was as follows: $0.03\ TiO_2 : 1\ SiO_2 : 25\ H_2O : 0.32\ TPAOH : 0.77\ i\text{-}PrOH$. This gel was then heated statically in Teflon-lined stainless steel autoclaves at autogeneous pressure at 170°C for 48 h. The resulting solid was recovered, washed with deionized water, dried, and calcined in static air at 550°C for 8 h to remove the template.

Large crystals of TS-1 (Si/Ti = 34) were synthesized according to the procedure of Milestone and Sahasrabudhe (9). A typical synthesis mixture consisted of 1 g of SiO_2 (Aerosil 200, Degussa), 0.5 g of TPABr (Fluka), 1.6 ml of a 40% solution of TPAOH (Alfa), 0.6 g of NH_4F (Merck), 0.05 g of $(NH_4)_2TiF_6$ (Aldrich), and 20 ml of deionized water. The salts and the TPAOH were dissolved in the water and Aerosil was added and mixed until a homogeneous gel was obtained. The synthesis mixture was autoclaved in Teflon-lined stainless steel autoclaves and heated statically at autogeneous pressure at 170°C for 48 h. After crystallization, the solid was recovered, washed with deionized water, dried, and calcined in static air at 500°C.

Aluminum-free Ti-Beta (Si/Ti = 40) was synthesized according to a procedure adopted by Blasco *et al.* (10) using a starting gel of the following molar composition: $1\ TiO_2 : 25\ SiO_2 : 14\ TEAOH : 8.6\ H_2O_2 : 189\ H_2O : 14\ HF$. In a typical synthesis, 40 g of tetraethylorthosilicate (TEOS, Aldrich) is hydrolyzed under stirring at room temperature in a solution containing 45.37 g of tetraethylammonium hydroxide (TEAOH, 35 wt%, Alfa), 6.40 g of H_2O_2 (35 wt% in water, Fluka), and 2.29 g of water. After addition of 1.75 g of tetraethylorthotitanate ($Ti(OEt)_4$, Alfa), the solution is stirred at room temperature until the ethanol formed is evaporated. Finally, 4.49 g of HF (48 wt%, Aldrich) is added and the yellow thick paste is loaded in Teflon-lined stainless steel autoclaves and heated at 140°C under rotation (60 rpm) for 20 days. The product obtained after the crystallization is filtered, washed with deionized water, dried, and then calcined at 550°C in static air for 8 h.

The alkali ($Na^+ + K^+$) content in all templates was less than 50 ppm as confirmed by AAS.

The external surface of TS-1, synthesized according to the method described by Tangaraj *et al.* (4), was silanized using a low-temperature deposition of tetraethoxysilane (TEOS, Aldrich) (7). Nitrogen carrier gas (100 ml(NTP)/min) was led through a TEOS-containing saturator at 15°C and passed for 1 h at 100°C in the up-flow mode over a fixed bed of TS-1 (particle size 0.1 μm), the space velocity being 2.43 mg/(g · min). Subsequently, TS-1 was flushed with pure N_2 (100 ml(NTP)/min) for 0.25 h, heated in air (100 ml(NTP)/min) at 5°C/min up to 500°C, and kept at this temperature for 2 h. This procedure was repeated up to 20 times.

2.2. Characterization of TS-1 by Adsorption

The adsorption of phenol, hydroquinone, and catechol in TS-1 was determined from water, methanol, and acetone as solvent using a batch and a chromatographic technique.

In the batch adsorption method, 0.1 g of zeolite catalyst was suspended at 25°C in 5 ml of a 5 wt% phenol–solvent solution. After adsorption equilibrium was established (24 h), a liquid sample was analyzed by gas chromatography. This allowed us to calculate the phenol partition coefficient, α, as the ratio of adsorbed phenol in the molecular sieve and solvent phase.

The experimental set-up and conditions for the liquid-phase chromatographic method have been described elsewhere (11).

Pore mouth narrowing due to silanization was investigated by a gas-phase chromatographic technique using an experimental set-up similar to that used by Denayer *et al.* (12), taking cyclohexane, 3-methyl-pentane, and toluene as tracer components.

A hydrocarbon pulse (typically 1–4 μmol of hydrocarbon vapor in N_2) was injected in a carrier gas (argon, 30 ml(NTP)/min), which was led over a 1 cm column (4 mm internal diameter) containing 0.05 g of parent or inertized zeolite powder. The column was mounted in a GC equipped with a FID detector. The response on the pulse was monitored at 175–275°C and the shifts in the first and second moments of the peaks were taken as a measure for changes in the sorption behavior of TS-1 on inertization.

2.3. *Physicochemical Characterization*

All samples were characterized for silicon–titanium content (AAS), crystallinity (XRD), crystal size and morphology (SEM), extraframework titanium (UV–VIS), and surface area (BET).

Powder X-ray diffraction spectra were taken by means of a Philips X'PERT diffractometer generating Cu$K\alpha$ radiation ($\lambda = 0.1542$ nm) operating at 40 kV and 25 mA. Scanning was done between 4 and 55° 2θ with a step size of 0.02° 2θ and 2.0 s counting time.

N_2 BET surface areas were determined on a Micromeritics ASAP 2000 apparatus. Prior to N_2 adsorption, the samples were calcined at 500°C and degassed at 88 K.

Electron micrographs were obtained using a Leica LEO S440 scanning electron microscope (SEM) with the accelerating voltage set at 40 kV. The stage tilt was set at 0°, the working distance and aperture size being 7 mm and 30 μm, respectively. Samples were mounted on aluminum stubs and coated with Au/Pd film.

The infrared spectra were run on a Nicolet 5ZDX FT-IR spectrometer at a resolution of 4 cm^{-1} using self-supporting wafers of the samples.

Diffuse reflectance UV–VIS spectra were recorded from 800 to 200 nm on a UV–Vis–NIR Varian Cary 5 spectrophotometer with a certified standard of Labsphere (SRS-99-010) as reference.

Atomic adsorption spectroscopy was done on a Varian Spectra AA-100, using solutions of 0.2 g of zeolite dissolved in HF–HCl mixtures.

2.4. *Catalytic Hydroxylation of Phenol*

Phenol hydroxylation was usually carried out at 60°C with magnetic stirring (1000 rpm) in a 24-ml glass batch reactor equipped with a Teflon sample port. After dissolution of 1.3 g of phenol (Aldrich) in 5 ml of the solvent, 0.13 g of TS-1 was added. To start the reaction 4.6 mmol of H_2O_2, i.e., 0.5 g of a 30 wt% aqueous solution (Merck), was added in a single portion. Representative samples (0.2 ml) of the vigorously stirred reaction mixture were withdrawn and analyzed using HPLC. The HPLC was equipped with a C_{18} reverse-phase column (Luna) using 25 vol% of acetonitrile in water as mobile phase and a Beckman 168 diode array detector operating at 280 nm. The resulting H_2O_2 content was monitored by means of a standard iodometric titration.

After reaction, the catalyst was recovered by filtration on a 0.45-μm millipore filter, extensively washed with deionized water and dried at room temperature. The tar content of the zeolite was then analyzed using a Stanton Redcroft STA 780 series thermal analyzer with a sample mass of 25 mg. For this analysis, the sample was heated in nitrogen (60 ml(NTP)/min) at 5°C/min to 150°C to desorb water. Subsequently, the carrier gas was changed to air (60 ml(NTP)/min) and the sample was heated at 5°C/min to 550°C and kept at this temperature for 4 h.

2.5. *Kinetic Modeling of Phenol Hydroxylation*

The data obtained in the phenol hydroxylation experiments were fitted in concentration–time profiles with the following second-order kinetic expressions, first order in both phenol and hydrogen peroxide:

$$\frac{1}{S}\frac{dC_{\mathrm{p}}}{dt} = -k_{\mathrm{p}} C_{\mathrm{p}} C_{\mathrm{O}} \tag*{[1]}$$

$$\frac{1}{S}\frac{dC_{\mathrm{O}}}{dt} = -k_{\mathrm{p}} C_{\mathrm{p}} C_{\mathrm{O}} - k_{\mathrm{d}} C_{\mathrm{O}} \tag*{[2]}$$

$$\frac{1}{S}\frac{dC_{\mathrm{c}}}{dt} = k_{\mathrm{c}} C_{\mathrm{p}} C_{\mathrm{O}} \tag*{[3]}$$

$$\frac{1}{S}\frac{dC_{\mathrm{h}}}{dt} = k_{\mathrm{h}} C_{\mathrm{p}} C_{\mathrm{O}} \tag*{[4]}$$

$$\frac{1}{S}\frac{dC_{\mathrm{a}}}{dt} = (k_{\mathrm{p}} - k_{\mathrm{c}} - k_{\mathrm{h}}) C_{\mathrm{p}} C_{\mathrm{O}}. \tag*{[5]}$$

The following symbols are used: p = phenol, c = catechol, h = hydroquinone, o = oxidant (H_2O_2), a = tar (aselective reactions), d = nonselective decomposition of oxidant, S = total surface area, and t = time.

3. RESULTS

3.1. *Characterization of the Titanium-Containing Molecular Sieves*

Figures 1A–1C show the scanning electron micrographs of the obtained crystallites. The physical characteristics of the synthesized materials are listed in Table 1. All samples were highly crystalline and showed a single UV–VIS absorption band at 215 nm pointing to the absence of extraframework TiO_2 in the samples. The small TS-1 crystallites show a cubic morphology with an average diameter of about 0.1 μm. The large crystallites of TS-1 were

TABLE 1

Physical Characteristics of TS-1 and Al-Free Ti-Beta

	TS-1 (small)	TS-1 (large)	Ti-Beta
Ti/Si,[a] mol/mol	0.03	0.03	0.025
XRD crystallinity,[b] %	100	100	100
d_{crystal},[c] μm	ca. 0.1	45 × 10 × 3	2–5
BET surface area, m^2/g	442	422	514
Internal surface area, m^2/g	360	417	506
External surface area, m^2/g	82	5	8

[a] Determined by chemical analysis.

[b] Compared to 100% crystalline standard.

[c] Determined by SEM.

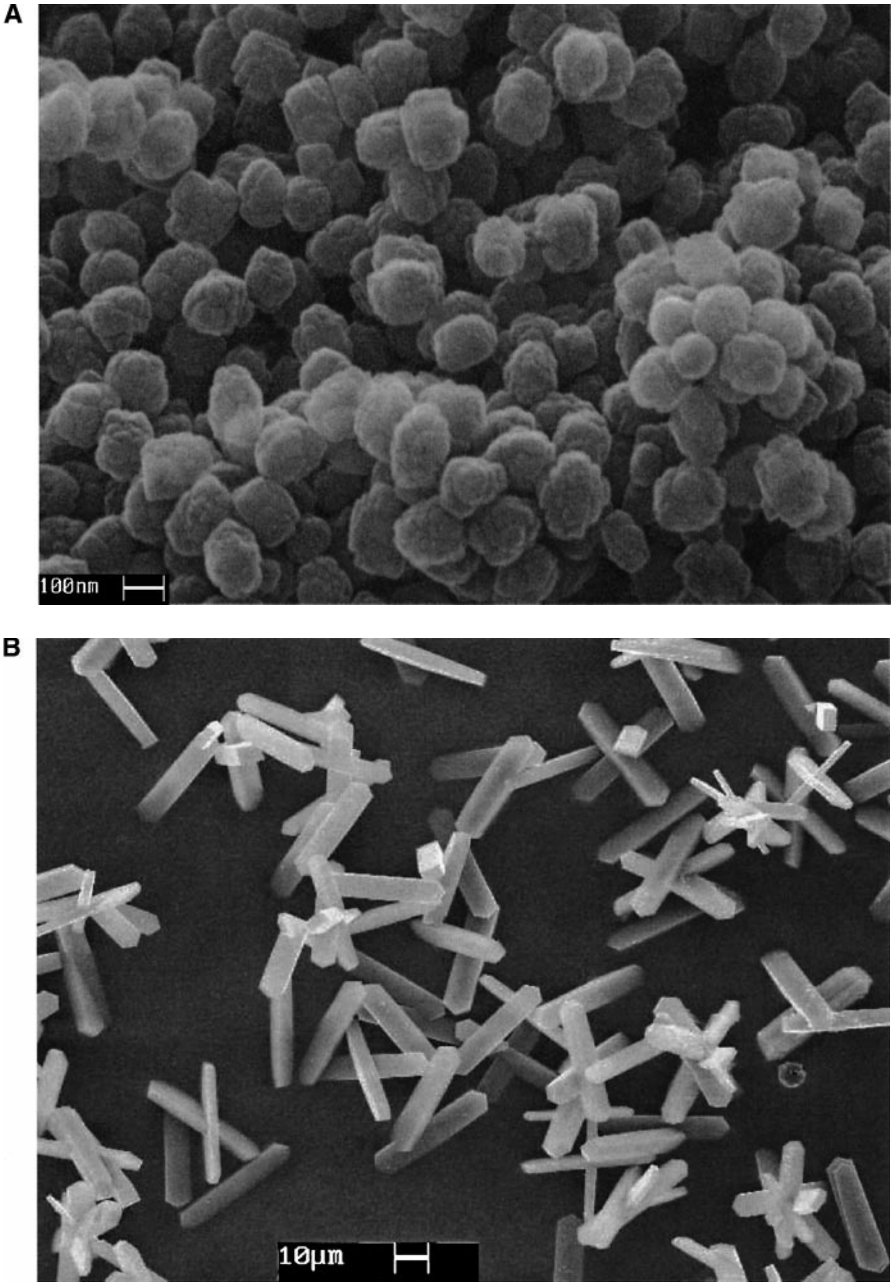

FIG. 1. Scanning electron micrographs of obtained titanium-containing molecular sieves. (A) Small crystals of TS-1; (B) large crystals of TS-1; (C) Al-free Ti-Beta.

coffin-shaped with dimensions of about 45 × 10 × 3 μm. With the straight channels of the zeolite structure being in the direction of the small axis ([010] direction) (13), the shortest diffusional path length is of the order of about 1.5 μm. The crystallites of Al-free Ti-Beta were well-faceted truncated square bipyramids of 2–5 μm. The diffusional path length in the large crystallites of TS-1 and Al-free Ti-Beta are thus similar, whereas the small TS-1 crystallites have a much shorter diffusional path length. The results obtained by BET for all samples are in agreement with literature (10, 16). For the small TS-1 crystals only ca. 82% of the total surface area is located in the pores of the crystal whereas the larger TS-1 and the Al-free Ti-Beta crystals have 98.5% of their Ti sites inside the pores.

The cyclic CVD procedure of TEOS is used to inertize the external surface of TS-1. However, depending on the silanization conditions, the application of this technique

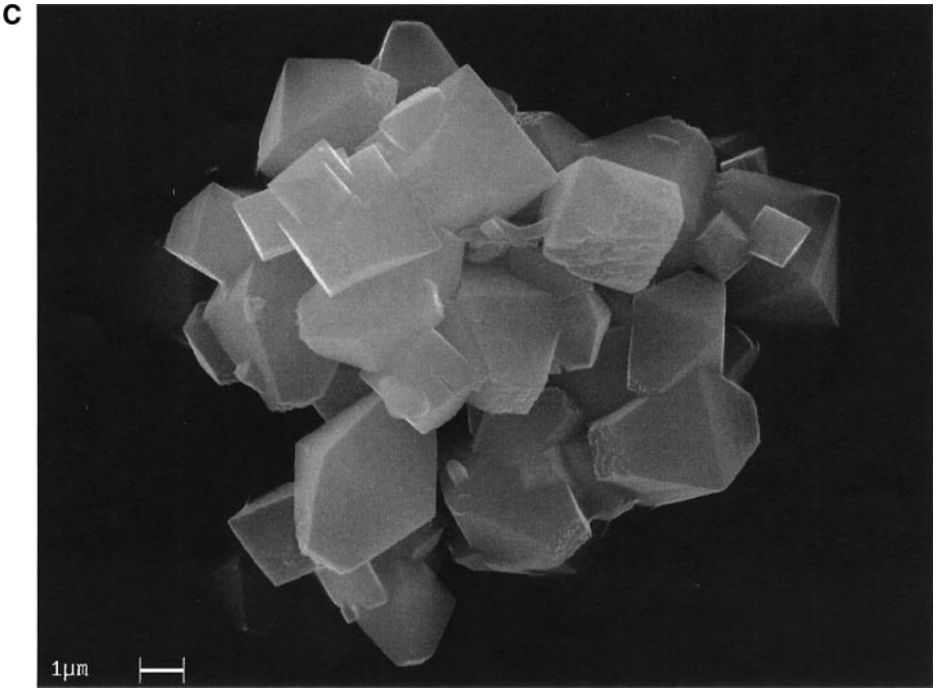

FIG. 1—*Continued*

can affect the zeolite pore mouth as well as result in pore mouth narrowing or blocking, as has been reported for ZSM-5 (7). The absence of pore mouth narrowing in the silanized TS-1 samples used in this work was confirmed by the chromatographic pulsed gas-phase sorption technique (12). No change in sorption properties (activation energy, first and second moment of pulse response) was observed for cyclohexane, 3-methyl-pentane and toluene. This confirms that the pore openings of the TS-1 samples were not significantly affected by the silanization procedure.

SEM pictures of parent and silanized TS-1 samples also showed no change, indicating that the agglomeration degree of the small crystallites also remained unchanged.

No significant changes in IR and UV–VIS spectra were observed. EDX of parent and silanized TS-1 showed an increase of the average Si/Ti ratio from 33 to 60, confirming the decrease of the Si/Ti ratio of the external rim of the crystals and thus the deposition of silica on the external surface.

3.2. *Phenol Hydroxylation*

The large difference in crystal size and thus in diffusional path length of the two TS-1 samples allows an investigation of the influence of diffusional constraints on the reaction. Furthermore, the small crystals have a much higher fraction of active Ti sites located on the external surface, which can yield information of the influence of the external surface on the reaction selectivities obtained. The large TS-1 and the Al-free Ti-Beta samples used in this work have a similar diffusional path length. The comparison of the phenol hydroxylation on both catalysts therefore yields information on the effect of the pore structure on the phenol hydroxylation (Table 2).

The phenol conversion over large crystals of TS-1 is lower than that over Al-free Ti-Beta. This can be attributed to the smaller pores of TS-1, showing that mass transfer controls the reaction rate. For the larger pores of Al-free Ti-Beta, intracrystalline diffusion is expected to be faster. With Al-free Ti-Beta catechol is the preferred product. This shows that the zeolite pore size controls the product formation. In the absence of a catalyst, only a low phenol conversion (0.85%) to tars was observed.

TABLE 2

Influence of the Zeolite Crystal Structure on the Phenol Hydroxylation in Water at 60°C and after 6 h under Standard Conditions[a]

Catalyst	X_{p}, %	X_{o}, %	H_2O_2 efficiency, %	Hydroquinone/ catechol ratio	Tar,[e] mg/g_{cat}
No catalyst	0.85	—	—	Only traces	—
TS-1[b]	5.8	18.3	71.5	1.3	n.d.[f]
Ti-Beta[c]	19.5	93.1	62.8	0.5[d]	118.0

[a] See Materials and Methods.
[b] TS-1 crystals of 3 × 10 × 45 μm.
[c] Al-free Ti-Beta of ca. 2–5 μm.
[d] Determined at X_{p} of 5.8%.
[e] Amount of tar deposited after 24 h reaction.
[f] Not determined (conversion not complete after 24 h).

TABLE 3

Influence of Crystal Size and External Surface Activity on the Phenol Hydroxylation over TS-1 in Water at 60°C and after 6 h under Standard Conditions[a]

$d_{crystal}$, μm	X_p, %	X_o, %	H_2O_2 efficiency, %	Hydroquinone/ catechol ratio	Tar[d] mg/g_{cat}
3 × 10 × 45	5.8	18.3	71.5	1.30	n.d.[e]
0.1	28.9	100	86.6	1.31[c]	84.2
0.1 (sil.)[b]	27.2	100	83.1	1.54[c]	53.0
0.1 (coked)	23.8	100	71.5	1.39[c]	91.5

[a] See Materials and Methods.

[b] Silanized small TS-1 crystals (20 CVD cycles).

[c] Values at 5.8% phenol conversion.

[d] Amount of tar deposited on TS-1 after 24 h.

[e] Not determined.

The effect of the crystal size and the role of the external surface for the phenol hydroxylation over TS-1 with water as a solvent are shown in Table 3. Silanization of small TS-1 crystals leads to a decrease in the amount of coke formed, pointing to a decreased activity of the external surface. Similar observations are noted for a coked TS-1 sample, which represents another way to achieve surface deactivation. A decrease in the crystal size of TS-1 leads to an enhancement in phenol and H_2O_2 conversion. This increase in the conversion cannot be attributed to the increase in the external surface, since under comparable conditions the conversion with the silanized sample of TS-1 is still significantly larger than that with the large crystals of TS-1. This suggests again that the phenol hydroxylation over large crystals is strongly diffusion limited. Van der Pol *et al.* (6) obtained a similar conclusion by comparing the activity of different crystal sizes of TS-1 in the phenol hydroxylation.

With increasing phenol conversion over TS-1, the hydroquinone-to-catechol ratio increases (Figs. 2 and 3). This can be the result of coke formation and poisoning of external surface sites (1). At similar phenol conversions the ratio of hydroquinone to catechol is independent of the crystal size (Table 3). Silanization of the external surface results in a further increase of the hydroquinone-to-catechol ratio. Catechol was, however, always formed in significant amounts. Even after a large number of silanization cycles the ratio of hydroquinone to catechol over TS-1 with water as a solvent never exceeded 1.8. This indicates that catechol is not only formed on the sites located on the external surface, but also in the pores of TS-1.

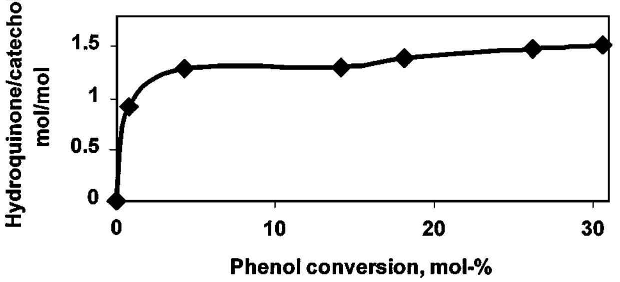

FIG. 2. Ratio of the amount of hydroquinone formed relative to the amount of catechol formed as a function of phenol conversion (phenol conversion varied by different reaction times); catalyst TS-1 ($d_{crystal} \approx$ 0.1 μm; $m_{catalyst}$ = 0.13 g; m_{phenol} = 1.3 g; 4.6 mmol of H_2O_2 (30% in water, 0.5 g of solution); 5 ml of H_2O as solvent).

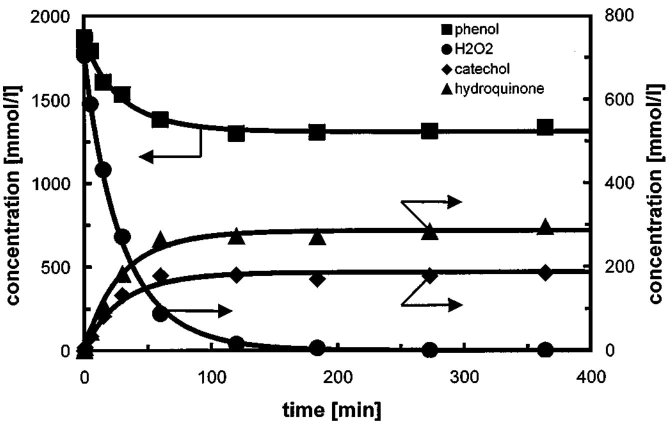

FIG. 3. Concentration–time profile in the phenol hydroxylation over TS-1 ($d_{crystal} \approx 0.1\ \mu$m; $m_{catalyst} = 0.13$ g; $m_{phenol} = 1.3$ g; 4.6 mmol of H_2O_2 (30% in water, 0.5 g of solution); 5 ml of H_2O as solvent).

In Fig. 3 the typical concentration–time profiles of reactants and products, as well as the fit of the kinetic model applied (Eqs. [1]–[5]), are given. A good fit was obtained for all experiments, showing that the overall second-order kinetic model describes the reaction well.

The influence of the solvent on the phenol hydroxylation is summarized in Table 4. The highest catalytic activity, expressed as k_p, is obtained with water as a solvent. This can be ascribed to the strong adsorption of phenol in TS-1 in this solvent, which is driven by the nonideality of the water–phenol solution. At the same mole fraction, the activity coefficient of phenol calculated using UNIFAC software (23) is much higher in water than in the other solvents (Table 5). Hence, high intraporous phenol and, as a result of competitive adsorption effects, low hydrogen peroxide concentrations are expected with water as a solvent. Surprisingly, no selectivity in the adsorption phenomena is observed in methanol and acetone. With methanol or acetone as a solvent the concentration of phenol in the pores is about the same, while the affinity of the zeolite phase is not much higher than that of the solution, as seen from the Henry's constants determined with the chromatographic technique (Table 6).

On the other hand, the catalytic activity of TS-1 in methanol is significantly higher than that obtained using acetone as a solvent, whereas peroxide efficiency is better in acetone as supported by the lower k_d values (Table 4). This might be attributed to the side reaction between acetone

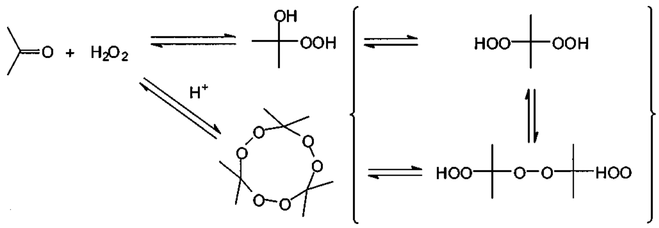

SCHEME 1. Formation of alkylidene peroxides from acetone and hydrogen peroxide (14).

and H_2O_2 yielding hydroxy hydroperoxy propane and derived products (14, 15) (Scheme 1), causing a lower concentration of free hydrogen peroxide at or near the active sites in the pores and a gradual release of free H_2O_2.

The hydroquinone selectivity is highest in methanol [see also (3)]. With acetone as a solvent the hydroquinone-to-catechol ratio is lowest and similar for the original TS-1 and Ti-Beta samples. This indicates that the selectivity of the reaction is governed much less by geometric constraints or otherwise stated that the reaction in acetone takes place to a larger extent on the external surface.

Tar formation is following a similar trend as phenol conversion (water > methanol > acetone). The tar deposition on the catalyst surface decreases when the tar components or precursors are more soluble in the solvent. On the other hand, the decrease in tar deposition upon silanization is only significant in water and negligible in acetone. The residual tar formation and hence deposition on silanized TS-1 catalysts is somewhat unexpected, but can be attributed to tar formation on titanium sites in pore mouths or even inside the micropores. The tar poisoning of active sites can be used as an alternative external surface inertization. Thus, a TS-1 sample was used for reaction in water (where the tar formation is most pronounced) and washed extensively with deionized water. When this coked sample was used for phenol hydroxylation in water (Table 3), no significant additional amount of tar is deposited (7.3 mg of tar/g of catalyst). However, a drastic decrease in phenol conversion (23.8%) was observed due to active site poisoning. The lower hydrogen peroxide efficiency (71.5%) observed is presumably related to side reactions between hydrogen peroxide and tar components.

TABLE 5

Phenol Partition (α) and Activity Coefficients (γ) in the Different Solvents

	α(TS-1)[a,b]	α(S-1)[a,c]	γ[d]
Water	33	19	9.0535
Methanol	≈1	—	0.5943
Acetone	≈1	—	0.3047

[a] See Materials and Methods: determined via both methods.
[b] TS-1 of 0.1 μm.
[c] Silicalite-1 of 0.2 μm.
[d] Calculated with UNIFAC under reaction conditions (60°C) (23).

The cyclic deposition of TEOS allows us to follow the progress of the inertization of the external surface. After a number of cycles, the catalyst was removed from the silanization reactor and used for a phenol hydroxylation experiment in water. Figure 4 shows the second-order rate constants for the phenol hydroxylation in water versus the number of silanization cycles. Due to the silanization the rate constant for the consumption of phenol is reduced by 42%. This is mainly attributed to the reduction in the formation of tars. The rate constant for the tar formation is reduced by 91%. The rate constant for hydroquinone formation decreases less than the rate constant of catechol formation (25 vs 35% reduction). This indicates that at the external surface the formation of catechol is favored over that of hydroquinone, confirming literature reports (3, 5). These results further point to the formation of at least some catechol inside the pores of TS-1, as its rate constant is not reduced to zero upon silanization.

4. DISCUSSION

4.1. Role of the External Surface—Kinetic Modeling

The present kinetic data enable us to determine the contribution of the external surface to the overall catalytic activity. The contribution of the external surface activity and the contribution of the sites in the pore system of the

TABLE 4

Influence of Solvent on the Observed Rate Constants for Phenol and Hydrogen Peroxide Consumption, Catechol, Hydroquinone, and Tar Formation in the Phenol Hydroxylation, as Well as the Tar Deposition of a Parent and Silanized TS-1 Sample

Solvent	k_p [l/(mol $\cdot$ m^2 $\cdot$ s)]	k_d [l/(m^2 $\cdot$ s)]	k_c [l/(mol $\cdot$ m^2 $\cdot$ s)]	k_h [l/(mol $\cdot$ m^2 $\cdot$ s)]	k_a^a [l/(mol $\cdot$ m^2 $\cdot$ s)]	Tar[b] [mg/g]	Tar[c] [mg/g]
Water	5.0×10^{-6}	2.0×10^{-3}	1.6×10^{-6}	2.5×10^{-6}	8.0×10^{-7}	84.2	53.9
Methanol	1.3×10^{-6}	1.1×10^{-3}	3.2×10^{-7}	6.9×10^{-7}	3.2×10^{-7}	57.0	46.1
Acetone	8.0×10^{-7}	5.5×10^{-4}	3.2×10^{-7}	2.6×10^{-7}	2.2×10^{-7}	47.0	46.7

Reaction at 60°C over TS-1 under standard conditions (see Materials and Methods).
[a] $k_a = k_p - k_c - k_h$.
[b,c] Tar deposition after 24 h reaction on parent and silanized TS-1 catalyst, respectively.

TABLE 6

Henry's Constants (K_i) for the Adsorption of Phenol (p), Hydroquinone (h), and Catechol (c) from Different Solvents in Small TS-1 Crystals As Determined by the Liquid-Phase Chromatographic Technique (11)

	Water	Methanol	Acetone
K_p	84.4	0.7	0.6
K_h	5.7	0.6	0.6
K_c	9.2	0.7	0.7

titanium containing molecular sieves can be evaluated as follows:

$$k_n S = k_{n,i} S_i + k_{n,e} S_e \qquad [6]$$

$$S = S_i + S_e, \qquad [7]$$

in which n stands for p, c, h, o, a; i for internal, e for external.

For the small TS-1 crystals, the total surface area (S) and the external surface area (S_e) were determined to be 442 m^2/g and 82 m^2/g, respectively. Assuming that after 20 cycles the role of the external surface in the phenol hydroxylation can be neglected; i.e., the observed activity is solely due to the activity of TS-1 in the pores, the contribution of the internal and external surfaces can be evaluated. The assumption of full inertization of the external surface of TS-1 after 20 cycles seems justified due to the relatively small changes in the rate constants (within the error of the method) between 15 and 20 cycles of TEOS deposition.

Table 4 shows the influence of the solvent on the overall rate constants. All observed rate constants reported are a product of the intrinsic rate constants and the sorption constants. The rate constants for the activity of the sites inside the pores of TS-1, obtained with a sample that has been exposed to 20 cycles of TEOS deposition, and the rate constants for the activity on the external surface obtained by applying Eq. [6] are given in Table 7.

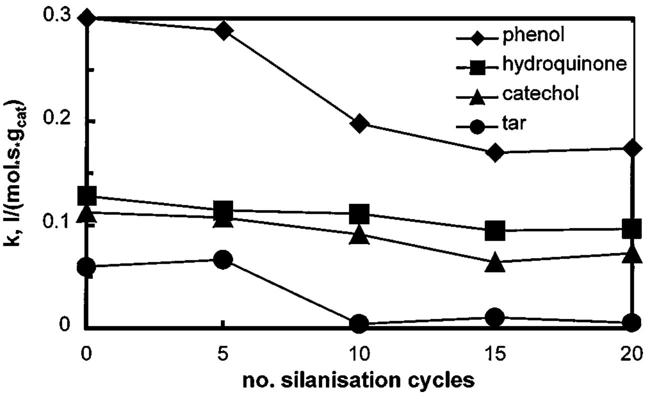

FIG 4. Overall rate constants for the consumption of phenol and the formation of catechol, hydroquinone, and tar in the phenol hydroxylation over TS-1 as a function of the number of cycles of deposition of TEOS ($d_{crystal} \approx 0.1\,\mu m$; $m_{catalyst} = 0.13$ g; $m_{phenol} = 1.3$ g; 4.6 mmol of H_2O_2 (30% in water, 0.5 g of solution); 30 ml of H_2O as solvent).

The observed rate constants for sites at the external surface are all larger than those at the internal surface. Principally, diffusional constraints could also account for the difference between the observed rate constants for sites at the external surface and those in the intracrystalline voids. The crystals of TS-1 used in these experiments were ca. 0.1 μm. Based on the diffusion coefficient of 2×10^{-18} m^2/s for phenol in TS-1 reported by van der Pol *et al.* (6), the effectiveness factor should be close to 1. Other diffusion measurements of phenol in various solvents with large TS-1 crystals, prior to exposure to hydrogen peroxide, yielded diffusion coefficients that are 2 orders of magnitude larger (17). Thus, the assumption of an effectiveness factor close to 1 for the small crystals seems to be justified.

On the basis of the rate constants determined for parent and inertized TS-1, the contributions of internal and external surface in different solvents can be evaluated (Table 7).

In water, the consumption of phenol mainly takes place on the external surface. The contribution of internal surface to the overall rate of phenol consumption amounts to

TABLE 7

Influence of Solvent on the Observed Rate Constants for Phenol and Hydrogen Peroxide Consumption and the Observed Rate Constants for the Formation of Catechol, Hydroquinone, and Tars in the Phenol Hydroxylation (Both Based on the Concentration in the Liquid) at 60°C over TS-1 ($d_{crystal} = 0.1\,\mu m$; $m_{catalyst} = 0.13$ g; $m_{phenol} = 1.3$ g; 4.6 mmol of H_2O_2 (30% in Water, 0.5 g of Solution); 5 ml of Solvent)[a]

Solvent		k_p [l/(mol · m^2 · s)]	k_d [l/(m^2 · s]	k_c [l/(mol · m^2 · s)]	k_h [l/(mol · m^2 · s)]	k_a[b] [(l/(mol · m^2 · s)]
Water	k_{ni}	1.9×10^{-6}(32)	1.1×10^{-3} (44)	7.2×10^{-7}(35)	1.2×10^{-6}(39)	1.1×10^{-8}(1)
	k_{ne}	1.8×10^{-5}(68)	6.0×10^{-3}(56)	5.7×10^{-6}(65)	8.2×10^{-6}(61)	4.3×10^{-6}(99)
Methanol	k_{ni}	8.8×10^{-7}(54)	6.3×10^{-4}(44)	2.1×10^{-7}(54)	6.1×10^{-7}(73)	5.6×10^{-8}(13)
	k_{ne}	3.3×10^{-6}(46)	3.4×10^{-3}(56)	7.7×10^{-7}(46)	1.0×10^{-6} (27)	1.5×10^{-6}(87)
Acetone	k_{ni}	4.1×10^{-7} (42)	1.8×10^{-4}(26)	1.3×10^{-7}(31)	1.4×10^{-7} (44)	1.5×10^{-7} (54)
	k_{ne}	2.5×10^{-6} (58)	2.2×10^{-3} (74)	1.2×10^{-6} (69)	7.9×10^{-7} (56)	5.5×10^{-7} (46)

[a] Values in parentheses represent percent contribution of total formation/consumption ($S \cdot k$).

[b] $k_a = k_p - k_c - k_h$.

TABLE 8

Rate Constant for the Formation of Hydroquinone (k_h) Relative to the Rate Constant for the Formation of Catechol (k_c) on the Internal Surface Sites and the External Surface Sites in Different Solvents (Catalyst, TS-1 ($d_{crystal} = 0.1\ \mu m$); $m_{crystal} = 0.13$ g; $m_{phenol} = 1.3$ g; 4.6 mmol of H_2O_2 (30% in Water, 0.5 g of Solution); 5 ml of Solvent; $T_{reaction} = 60°C$)

	Water	Methanol	Acetone
k_{hi}/k_{ci}	1.68	2.90	1.07
k_{he}/k_{ce}	1.43	1.29	0.66

only 32%. The small contribution of the internal surface to the rate of consumption of phenol can be explained by the strong adsorption of phenol in TS-1 using water as a solvent. Due to competitive adsorption, the hydrogen peroxide concentration near the active sites inside the pore system of TS-1 (internal surface) will be very low. This will result in a low observed rate for the consumption of phenol in the pores.

With both methanol and acetone as a solvent the internal surface contributes to the overall rate of consumption of phenol for 54 and 42%, respectively. The difference between methanol and acetone can be explained by the formation of acetone peroxides and hydroperoxides (14, 15) (Scheme 1), which are too bulky to react with titanium sites in the pores. This is supported by the fact that TS-1 is very poorly active for oxidation reactions when *tert*-butylhydroperoxide is used as an oxidant. The formation of these compounds thus lowers the concentration of free hydrogen peroxide in the liquid phase and consequently in the pores of TS-1. Thus, in acetone the internal surface contributes less to the overall reaction compared to the reaction done in methanol.

On the basis of the rate constants obtained for hydrogen peroxide decomposition on silanized and nonsilanized TS-1 (Table 7), the contribution of the external surface to the rate of the nonselective hydrogen peroxide decomposition, k_d, for both methanol and water as a solvent amounts to 56%. With acetone as a solvent this amounts to 74%, as a consequence of the formation of the acetone peroxides resulting in a lower concentration of hydrogen peroxide in the pores of TS-1. The rate constant for the nonselective decomposition of hydrogen peroxide with water and methanol as a solvent is 5.5 times larger on the external surface. With acetone as a solvent this rate constant is 12 times larger than that for the internal surface. In all solvents, the homogeneous decomposition of hydrogen peroxide was found to be negligible for the duration of the experiment.

The contribution of the external surface to the rate of formation of catechol is significant. Depending on the solvent, the contribution of the external surface to the total rate of catechol formation varies between 46 and 69%. For the formation of hydroquinone, the contribution of the external surface sites to the total rate of formation of hydroquinone is dependent on the solvent nature. With water as a solvent, the contribution of the external surface sites to the total rate of formation of hydroquinone amounts to 60% (for the formation of catechol this is 66%). This clearly indicates that with water as solvent the reaction mainly takes place on the external surface sites, which can be explained by the strong adsorption of phenol and the consequently low hydrogen peroxide concentration in the zeolite pores. With methanol or acetone as a solvent, the contribution of the external surface sites to the total rate of formation of hydroquinone amounts to 27 or 56%, respectively. The catechol selectivity is 45 and 68% in methanol and acetone, respectively.

The kinetic data also contain information on the ratio of the activity of the internal and external surface sites for the formation of catechol and hydroquinone (Table 8). In all solvents, on the internal surface titanium sites hydroquinone is preferentially formed. This can be attributed to a geometric constriction for the reaction taking place in the pore system of a titanium silicalite-1 catalyst. This is in line with the observation that at 5.8% phenol conversion over large crystals of TS-1 and Al-free Ti-Beta in water, a hydroquinone-to-catechol ratio of 1.3 and 0.5, respectively, was observed. On the external surface sites, a particular solvent effect is observed. In protic solvents (water and methanol) hydroquinone formation is preferred over catechol formation. In acetone, as an aprotic solvent, the observed distribution is statistical.

Decoupling internal and external surface activity clearly demonstrates that the majority of the tar formation is taking place at the external surface of the zeolite. Especially with water as a solvent the external surface contributes 99% to the total rate of formation of tars.

4.2. *Mechanistic implications*

TS-1- and Al-free Ti-Beta-catalyzed phenol hydroxylation are possible only with hydrogen peroxide as the oxidant. Even though the organic peroxides such as *tert*-butylhydroperoxide may not penetrate the pores of TS-1 there is ample space in the pores of Ti-Beta to activate the Ti sites, as is well known for epoxidation reactions (10). However, no phenol hydroxylation occurs when *tert*-butylhydroperoxide is used as the oxidant. This strongly indicates that the aromatic hydroxylation over titanium-substituted molecular sieves follows a different reaction mechanism than epoxidation reactions. Hence, it is proposed that the terminal OH of the titanium hydroperoxo group is the electrophile that attacks the aromatic ring, similar to the mechanism for amine hydroxylation, as suggested by Reddy and Jacobs (18). However, the existence of other pathways, e.g., through the formation of radicals,

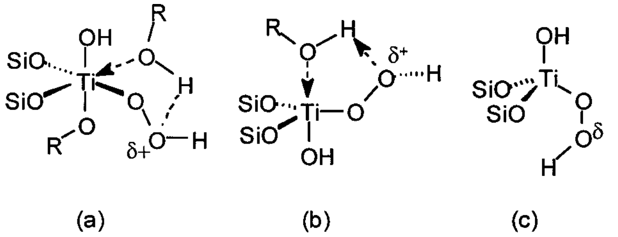

SCHEME 2. Possible configurations of the hydroperoxo-titanium active site of TS-1: (a) hexacoordinate octahedral, (b) pentacoordinate trigonal bipyramidal, and (c) tetracoordinate tetrahedral.

cannot be excluded. The differences in pore size of the two tested molecular sieves reflect the difference in the product selectivity of phenol hydroxylation with H_2O_2. As reported earlier, in the narrow pores of TS-1 hydroquinone formation is favored over that of catechol, whereas for Al-free Ti-Beta the relative amount of catechol is close to the statistical distribution.

When the external surface of TS-1 was inertized with SiO_2, a relatively high amount of *o*-hydroxylation was detected. The ratio of hydroquinone to catechol is always lower at the external surface than at the internal surface. This can be rationalized by the fact that at the external surface the geometric constrictions are low and *o*-hydroxylation becomes more likely. This does not mean that in the narrow TS-1 pores catechol formation is excluded.

To understand *para* or *ortho* hydroxylation, attention must be focused on the titanium sites. The interaction of protic solvents, such as alcohols and water, with Ti sites is well known and confirmed by spectroscopic studies. In literature, it is generally agreed that protic molecules coordinate to titanium, expanding its coordination sphere to 5 or 6 (19, 20). An increase in the average Ti–O bond length upon adsorption of methanol and water has been observed as well (20). A five-membered ring with hydrogen bonds between methanol and the peroxo group at the titanium site has often been proposed as the active intermediate complex for TS-1 catalyzed reactions (2, 21). Scheme 2 shows possible configurations of the titanium active site without (species **c**) and with coordination of 1 or 2 protic solvent molecules (species **a** and **b**).

The coordination of protic solvent molecules results in an increase of the size of the active titanium site. This narrows the TS-1 channels, leading to a geometric constraint for an approaching phenol molecule. Hydrogen bonds of the phenolic OH with solvent OH groups will make the phenol molecule more bulkier. Phenol, hydrogen-bonded to the solvent OH groups, will approach the bulky titanium site with the OH group pointing away from the titanium site (Scheme 3) yielding hydroquinone. Additionally, the presence of coordinated protic molecules close to the peroxo group could lead to hydrogen bond formation with the active site (species **a** and **b** in Scheme 2), destabilizing H-bonding with the phenol molecule assisting in *o*-hydroxylation (as shown in Schemes 4A and 4B).

On the other hand, in nonprotic solvents, phenol can take over the role of the protic solvent molecule. Although water is always present, its concentration in the hydrophobic TS-1 pores is expected to be low, as indicated by the extremely high *K* value of phenol in TS-1 with water as a solvent. Thus, the existence of titanium sites without protic molecules coordinated is proposed (Scheme 2, species **c**). In that case another reaction pathway is opened, i.e., the conversion via pentacoordinated (trigonal bipyramidal) Ti site, involving coordination of phenol to Ti peroxo species yielding catechol (Scheme 4A). This will be the case in aprotic solvents, such as acetone. Protic solvents will compete with phenol, so that this pathway is not dominant in these solvents.

Formation of catechol without coordination of phenol to the active titanium site takes place via a six-membered transition state involving phenol (see Scheme 4B).

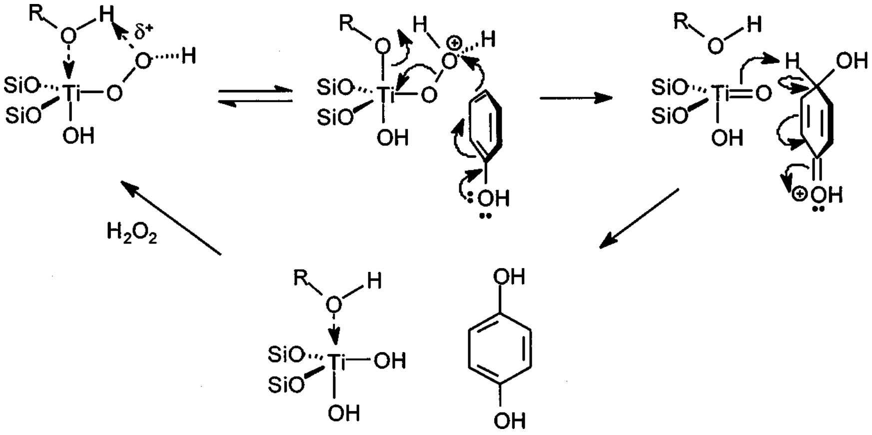

SCHEME 3. Proposed reaction mechanism for the formation of hydroquinone in phenol hydroxylation.

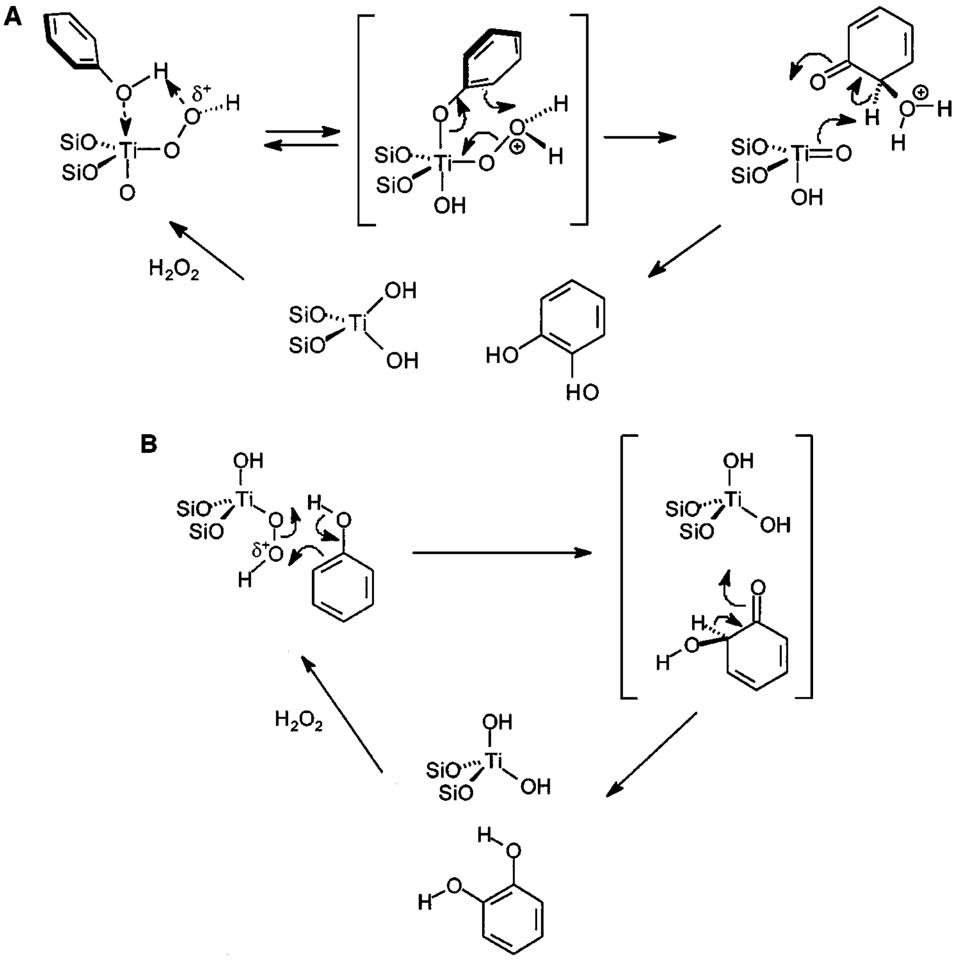

SCHEME 4. Proposed reaction mechanism for the formation of catechol in phenol hydroxylation.

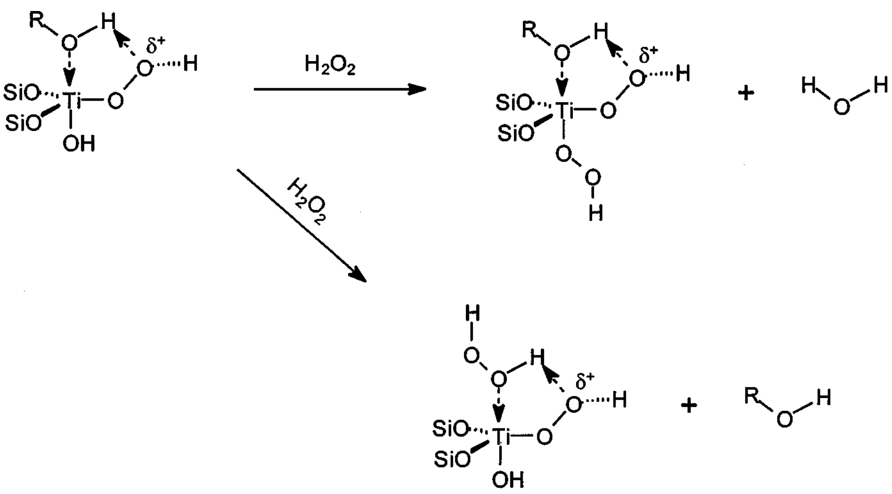

SCHEME 5. Proposed titanium sites on the external surface of TS-1.

Summarizing, hydroquinone is formed in a more selective way under limiting geometric conditions, as in the pores of TS-1, and strongly influenced by H-bonding effects of polar solvents. On the other hand in apolar solvents or for less restricted geometric Ti sites, as in the outer surfaces or in wider-pore molecular sieves, catechol will be the preferred product.

The formation of tars takes place mainly outside the TS-1 channels, since only a limited decrease in catalytic activity is observed in a regeneration experiment. Due to the hydrophobic nature of the TS-1 pores, a relatively low level of H_2O_2 is expected inside the pores, especially in water. At the external surface, titanium is exposed to much higher peroxide concentrations and the formation of a second OOH group at the same titanium atom may take place; the existence of titanium di(hydro)peroxo species has been postulated (22). Alternatively, H_2O_2 molecules could compete for coordination at the titanium peroxo site (Scheme 5). These rather unstable complexes could liberate singlet molecular oxygen that is quenched to its triplet state (22) and hence decrease the oxidant selectivity and lead to overoxidation and thus coke formation. These particular external sites are poisoned with the tars as the reaction progresses, explaining the shift toward the production of more hydroquinone relative to catechol with time in water and methanol. Since acetone is a good solvent for tars, the poisoning of these sites is prevented and no shift toward more hydroquinone is observed.

CONCLUSION

The conversion of phenol in the presence of hydrogen peroxide is determined by the pore geometry, the external surface titanium sites, the crystal size of the titanium-containing molecular sieve, and the nature of the solvent. Smaller pore dimensions (TS-1 vs Al-free Ti-beta) lead to a decreased conversion and an enhanced selectivity for hydroquinone. The phenol hydroxylation is strongly diffusion limited and small crystals should be applied. With small crystals the external surface sites contribute significantly to the total rate of reaction and its selectivity.

Especially in water as a solvent, a significant part of phenol conversion is due to external surface activity. While in the pores of TS-1, hydroquinone is clearly the preferred product, the major product formed on the external surface is solvent dependent: catechol is preferred in acetone, hydroquinone in protic solvents. In protic solvents, the coordination of solvent molecules to the titanium peroxo site leads to a geometric constraint in the TS-1 pores, inducing a “transition-state shape selectivity” with the para isomer preferentially formed.

ACKNOWLEDGMENTS

We thank K. Vanlaere for some of the experiments on the phenol hydroxylation. The cooperation between the Katholieke Universiteit Leuven, Vrije Universiteit Brussel, and University of Cape Town was sponsored by the Flemish and South African governments in the frame of an international scientific and technological cooperation. The Flemish partners acknowledge IUAP-PAI for sponsoring as well. Financial assistance from NRF and THRIP (South Africa) is greatly acknowledged. We thank I.W.T (F.v.L.) and IUAP-PAI (G.L.) for fellowships.

REFERENCES

1. Romano, U., Esposito, A., Maspero, F., Neri, C., and Clerici, M., *Stud. Surf. Sci. Catal.* **55**, 33 (1990).
2. Martens, J. A., Buskens, Ph., Jacobs, P. A., van der Pol, A., van Hooff, J. H. C., Ferrini, C., Kouwenhoven, H. W., Kooyman, P. J., and van Bekkum, H., *Appl. Catal. A* **99**, 71 (1993).
3. Tuel, A., Moussa-Khouzami, S., Ben Taarit, Y., and Naccache, C., *J. Mol. Catal.* **68**, 45 (1991).
4. Tangaraj, A., Kumar, R., Mirajkar, S. P., and Ratnasamy, P., *J. Catal.* **130**, 1 (1990).
5. Thangaraj, A., Kumar, R., and Ratnasamy, P., *J. Catal.* **131**, 294 (1991).
6. van der Pol, A. J. H. P., Verduyn, A. J., and van Hooff, J. H. C., *Appl. Catal. A* **92**, 113 (1992).
7. Röger, H. P., Krämer, M., Möller, K. P., and O’Connor, C. T., *Microporous Mesoporous Mater.* **21**, 607 (1998).
8. Wang, I., Ay, C.-L., Lee, B. L., and Chen, M.-H., “Proceedings, 9th International Congress on Catalysis, Calgary, 1988” (M. J. Philips and M. Ternan, Eds.), p. 324. Chem. Institute of Canada, Ottawa, 1988.
9. Milestone, N. B., and Sahasrabudhe, N. S., “Proceedings of the 12th International Zeolite Conference” (M. M. J. Treacy, B. K. Marcus, M. E. Bisher, and J. B. Higgins, Eds.), p. 1901. MRS, Warrendale, 1999.
10. Blasco, T., Camblor, A., Corma, A., Esteve, P., Guil, J. M., Martinez, A., Perdigon-Melon, J. A., and Valencia, S., *J. Phys. Chem. B* **102**, 75 (1998).
11. Langhendries, G., De Vos, D. E., Baron, G. V., and Jacobs, P. A., *J. Catal.* **187**, 453 (1999).
12. Denayer, J. F., Souverijns, W., Jacobs, P. A., Martens, J. A., and Baron, G. V., *J. Phys. Chem. B* **102**(23), 4588 (1998).
13. Ruthven, D. M., Eic, M., and Richard, E., *Zeolites* **11**, 647 (1991).
14. Davies, A. G., “Organic Peroxides.” Butterworth, Stoneham, MA, 1961.
15. Sauer, M. C. V., and Edwards, J. O., *J. Phys. Chem.* **75**(19), 3004 (1971).
16. Mirajkar, S. P., Thangaraj, A., and Shiralkar, V. P., *J. Phys. Chem.* **96**, 3073 (1992).
17. Wilkenhöner, U., Duncan, W., and van Steen, E., in preparation.
18. Reddy, J. S., and Jacobs, P. A., *Catal. Lett.* **37**, 213 (1996).
19. Bonneviot, L., Trong On, D., and Lopez, A., *J. Chem. Soc., Chem. Commun.* 685 (1993).
20. Davis, R. J., Liu, Z., Tabora, J. E., and Wieland, W. S., *Catal. Lett.* **34**, 101 (1995).
21. Bellussi, G., Carati, A., Clerici, M. G., Maddinelli, G., and Millini, R., *J. Catal.* **133**, 220 (1992).
22. van Laar, F. M. P. R., De Vos, D., Vanoppen, D. L., Pierard, F., Brodkorb, A., Kirsch-De Mesmaeker, A., and Jacobs, P. A., “Proceedings of the 12th International Zeolite Conference” (M. M. J. Treacy, B. K. Marcus, M. E. Bisher, and J. B. Higgins, Eds.), p. 1213. MRS, Warrendale, 1999.
23. Sandler, S. I., “Chemical and Engineering Thermodynamics,” 2nd Ed. Elsevier, Amsterdam, 1992.